STEREOGRAPHIC VIRTUAL REALITY REPRESENTATIONS OF MICROFOSSILS IN LIGHT MICROSCOPY

Michael W. Knappertsbusch

Michael.Knappertsbusch. Natural History Museum Basel, Augustinergasse 2 4001-Basel, Switzerland. Michael.Knappertsbusch@unibas.ch

ABSTRACT

A method is developed to produce animated stereographic representations of microfossils seen through a binocular at full-focal resolution by means of computer-assisted light microscopy. Stereopair images were obtained using a special stand for the binocular microscope that allows users to acquire a pair of images from slightly different angles of view at the same focal plane. Increased depth of focus was possible with the application of a special macro available from the NIH-image software library. Quantitative relationships between the working distance of the objective lens to object, and the parallax displacement of the resulting images on the computer monitor are given. These are useful in generating images at improved depth of focus. Three-dimensional animations were created from sequences of stepwise changing aspects of the object and from various focal levels, that were combined into a moving representation using Quick-Time Virtual Reality Authoring Studio from Apple Computer, Inc. A special eucentric specimen holder was designed in order to take images of the same object under varying orientations. The method is well suited to illustrate microfossils in the size range between 100 to 1000 μm and is a useful new technology for teaching purposes, construction of illustrated type-specimen databases, and for the display of microfossils to a general audience in museum exhibitions.

INTRODUCTION

Paleontologists often suffer from limited access to prime reference materials for taxonomic studies because the necessary materials are unique and rare. Frequent handling is discouraged to minimize the risk of damage or loss. In such situations, the researcher needs to consult literature and atlases where the specimens are described and illustrated. In traditional taxonomic monographs specimens are presented in two-dimensional (2D) photographs, usually in front view, side view, and back view, often with additional enlargements to illustrate morphological details. In some cases it may be advantageous if the structures could be shown in three dimensions (3D) or as an animation to better understand the anatomy of a

shell. Of course, sophisticated imaging techniques such as scanning of the topography with a laser beam, X-ray computer tomography, or photogrammetric methods have been developed. In recent years these once esoteric computer reconstruction techniques have become more available, most of them for macroscopic applications. Examples can be found in disciplines from medical surgery to paleoanthropology and in paleontology (Sutton et al. 2001; Zollikofer et al. 1998; Zollikofer and Ponce de Léon 2000, Ponce de Léon and Zollikofer 2001). Impressive examples for Neanderthal skull reconstructions, for example, can be found at the Anthropological Institute of the University of Zürich under the URL http://www.ifi.unizh.ch/staff/zolli/CAP/Main_face.htm. For microscopic applications, however, these techniques are limited. Lyons and Head (1998) presented a 3D visualization technique, that can be applied to scanning electron photomicrographs. For light microscopy, a similar approach is complicated by limited depth of field, which causes unsharp regions to appear in the images.

This latter problem is addressed in the present report. A method is presented herein to illustrate microscopic objects in the 100 µm to 1000 µm size range under reflected light in 3D stereo view, at extended depth of focus. In addition, collections of such images can be animated, so that the object can be observed from all sides on a computer monitor. Planktonic foraminifers (marine pelagic, calcite shell-secreting protists) were used to illustrate the technique, but the method can easily be applied to other microfossils (e.g., radiolarians, benthic and larger foraminifera, ostracods).

The method was developed using a Leica binocular microscope mounted on a AX microscope carrier. The up-and-down movement of the objective during focusing was measured with an electronic precision caliper. Stereo-pair images were taken at a series of subsequent focal planes with a digital video camera. Applying this technique to a series of images from varying positions, and using commercial virtual reality software allowed generation of an animation for 3D stereographic view of the microfossil at extended focal resolution.

This technique is ideal to illustrate unique type specimens in three dimensions. The method may also be used to construct digital taxonomic atlases or illustrated micropaleontological databases. Another obvious application involves the preparation of computer animations of microfossils for teaching purposes or oral presentations, animations in public displays, and exhibition of microfossils in museums.

Figure 1. 1. Imaging station used for the present study. See Figure 1B for digital dial gauge, which is mounted on the back side of the binocular microscope (red arrow) and allows the user to measure the vertical displacement of the lens-system during focusing. **1.2.** Digital dial gauge to measure the vertical displacement of the lens-system during focusing. The arrow points to the contact between the fixed part of the stand (black) and the moving part of the binocular microscope (white).

EQUIPMENT AND MATERIALS

Test Objects

The experiments were realized using Recent foraminiferal ooze from the Mediterranean Sea (sample Ki04, 0-1.5 cm from French VICOMED I expedition; see Knappertsbusch 1993) and a specimen of the planktonic foraminifer, *Globorotalia menardii*, Parker, Jones, and Brady, obtained by standard wet-sieving methods, from the top of Deep Sea Drilling Core 502A, sample 502A-1H-1, 15-20 cm (Holocene to upper Pleistocene), size fraction 500-1000 µm.

Hardware

For image acquisition a CCD color video camera (Kappa model CF 11/2) mounted on a Leica MZ 6 binocular microscope with a zoom magnification changer and connected to a Power Macintosh 8500/120 MHz with 130 MB RAM was used (e.g., Figure 1.1-1.2). The camera was delivered with a single 1/2" chip. Gray-level images (8-bit) were taken at 640x480 pixel spatial resolution. A standard magnification of 2.5x was applied to all images. This translates to a calibration factor of 0.300 pixels per µm in horizontal and 0.2989 pixels per µm in vertical direction on the final images.

Microscope Specifications:

The binocular microscope was equipped with a Leica AX stand, that allows the user to choose between stereoscopic and monoscopic vision. For stereoscopic vision the microscopist sees the object through the left and the right oculars perceiving a stereo-effect (e.g., Figure 2.1). In monoscopic vision the object is seen only through a
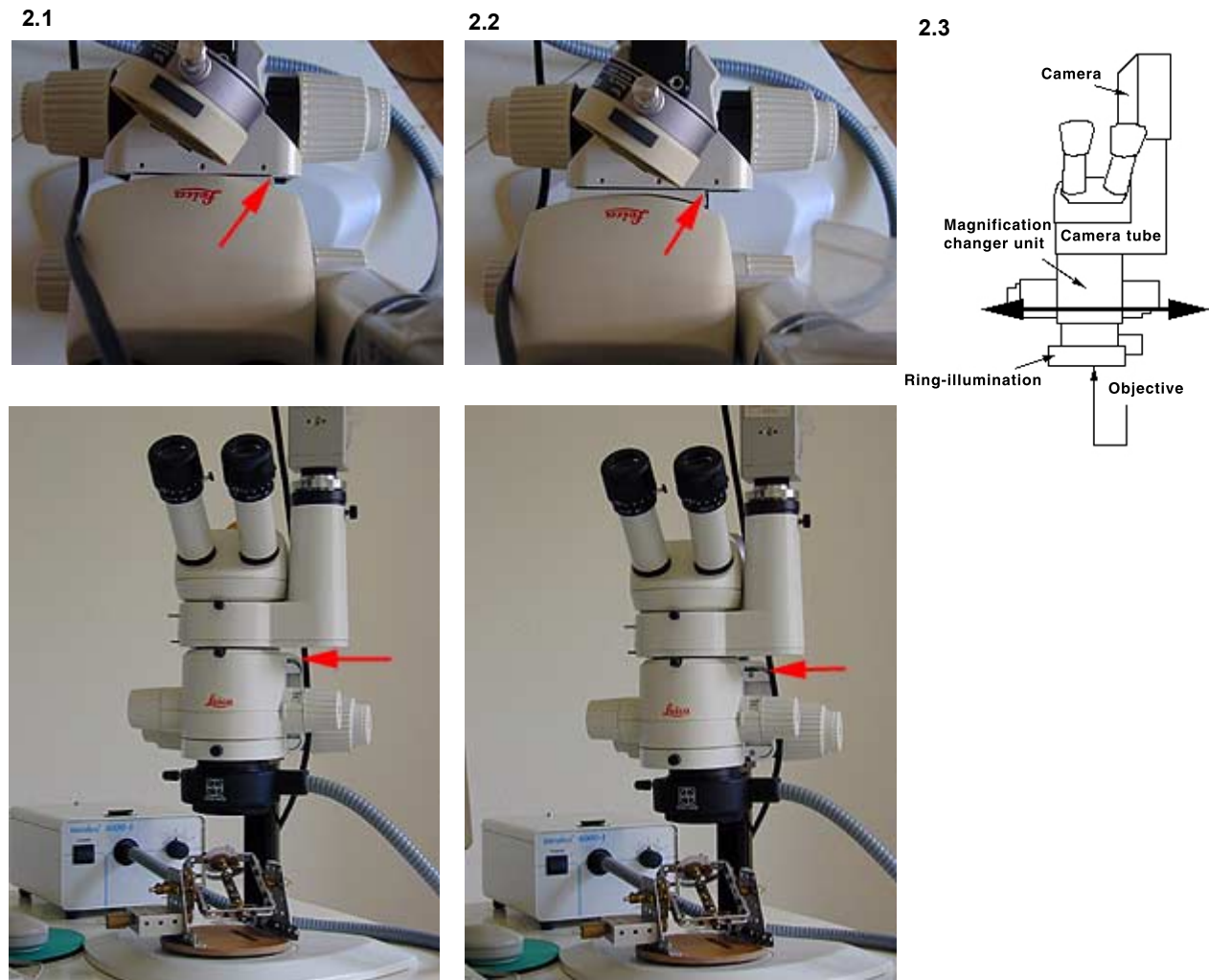
2.1

2.2

2.3

Figure 2. Stereoscopic and monoscopic positions of the magnification changer unit (red arrows point to the different positions). The magnification changer is the unit between the microscope objective (here surrounded by the black ring illumination) and the camera tube unit. **2.1.** Magnification changer unit in stereoscopic position, seen from above (upper panel) and in front view (lower panel). **2.2.** Magnification changer unit shifted to the left into monoscopic or coaxial position, seen from above (upper panel) and in front view (lower panel). **2.3.** Diagram of the microscope. The thick arrow indicates the movement of the microscope body for stereoscopic and monoscopic positions.

single light path (e.g., Figure 2.2), thus negating the stereo effect. These two modes can be manually chosen by shifting the magnification changer sidewards (e.g., Figures 2.1 and 2.2). In contrast to human vision the camera sees only in the monoscopic vision mode. When the magnification changer unit is set to the stereoscopic vision position, only light of the right image is deflected to the camera sensor (in this case the camera tube is mounted to the right side of the microscope body). This light beam is inclined with respect to the axis of up-and-down movement of the microscope for focusing. As a consequence, when moving the microscope up-and-down, the live video image on the computer monitor shifts sidewards. However, this displacement can be mechanically compen-

sated for when the magnification changer unit is switched to the left in monoscopic vision position. Then, the camera senses only the left light beam which is parallel to the vertical movement during focus operation, and the life image reproduced on the computer monitor remains stable. Images taken at identical focal planes but in stereo- and in mono positions form a stereo pair, which include a parallax displacement.

When focusing in the stereoscopic vision position, the horizontal shift of the image reproduced on the computer monitor is a function of the magnification and the vertical displacement of the microscope body. At constant magnification the relationship between image shift (*x*-dimension) on the monitor and the vertical position of the micro-
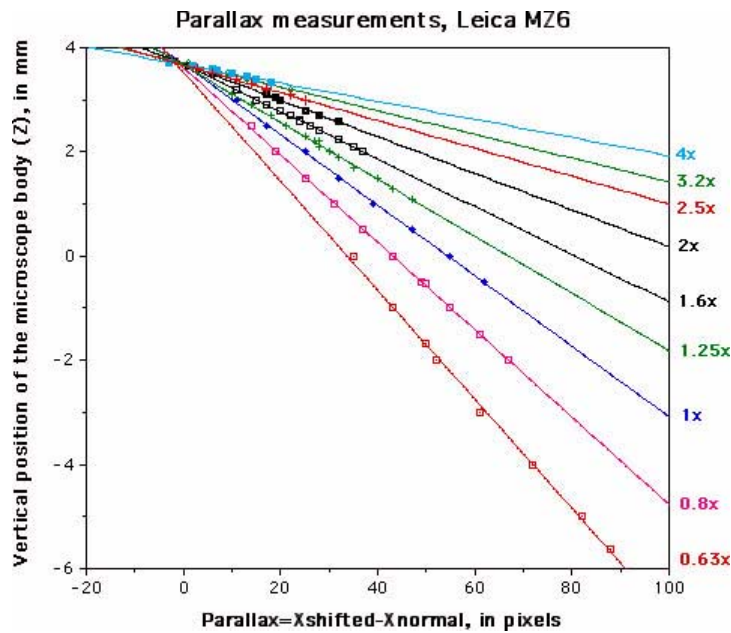
Figure 3. Relationship between the parallax displacement (Dx, in pixels) on the computer monitor and the relative vertical position of the magnification changer unit (z, in mm) for various magnifications (indicated in color for each line at the right side of the graph, see Equation 1 in the text). A 1x objective lens was used throughout for these experiments. The parallax displacement Dx is determined as the distance of pixels for an identical point in the image seen on the computer monitor between stereo-vision and mono-vision position at the same focal plane. The coefficients for the linear equations at each magnification are indicated in **Table 1.**

scope in focus position (z-dimension) becomes linear:

$$z = m * x + b \qquad \text{(Equation 1, see Fig. 3)}$$

The coefficients m and b are constants, which depend on the selected magnification (MAG) (e.g., Table 1 and Fig. 4). Note, that z is a direct measure of the working distance (focal length) of the lens system. The relative vertical position of the focal planes (z, in mm) was determined with a Sylvac digital dial gauge (precision 5 µm), that was mounted on a fixed part of the microscope and which records the vertical displacement of the microscope body during focusing (Fig. 1.2). The parallax (x, in pixels) is the difference of the x-coordinates of an identical point in the right (= stereo vision position) and the left (= mono or coaxial position) image. For the construction of animations all images were taken at a constant magnification (2.5x), and the parallax compensation for image shifts at different focal planes is then determined by the following formula:

$$x = Abs (z) / 0.002667 \qquad \text{(Equation 2)}$$

In Equation (2) x is the shift of a point in pixels seen at two different focal planes, which are separated at a vertical distance of z (in millimeter).

Microscope stage and orientation control

For the construction of animated scenes a series of images of the test object must be taken at constant steps of changing orientation. For this purpose a universal stage was constructed, that provides users with the ability to rotate manually

Table 1. Linear coefficients m and b for the lines illustrated in Figure 3 for magnifications 0.63x through 4x. The lines follow the linear equation y = m * x + b, where x denotes the parallax in pixels, and y is the vertical position of the microscope body (Z), in mm.

Microscope magnification	m	b
4x	-1.7419 e-2	3.6765
3.2x	-2.2768 e-2	3.7095
2.5x	-2.6671 e-2	3.6746
2x	-3.5167 e-2	3.7022
1.6x	-4.5770 e-2	3.6971
1.25x	-5.4727 e -2	3.6648
1x	-6.7683 e-2	3.6866
0.8x	-8.3897 e-2	3.6208
0.63x	-1.0464 e-1	3.5291

and tilt the object into any desired orientation (e.g., Figures 5.1-5.2 and 5.3-5.5). The foraminiferal specimen was fixed on the tip of a fine screw with a few drops of water-soluble glue. Small goniometric scales were attached to the moving parts of the stage so that orientation experiments could be repeated. The precision of this "archaetype" is less than 3°, which, while not impressive, was nevertheless good enough for the generation of the movie scenes shown herein.

Software

Wayne Rasband's NIH-Image 1.6.0 software was used to acquire digital images, process them,

Relationship between magnification and slope of parallax lines
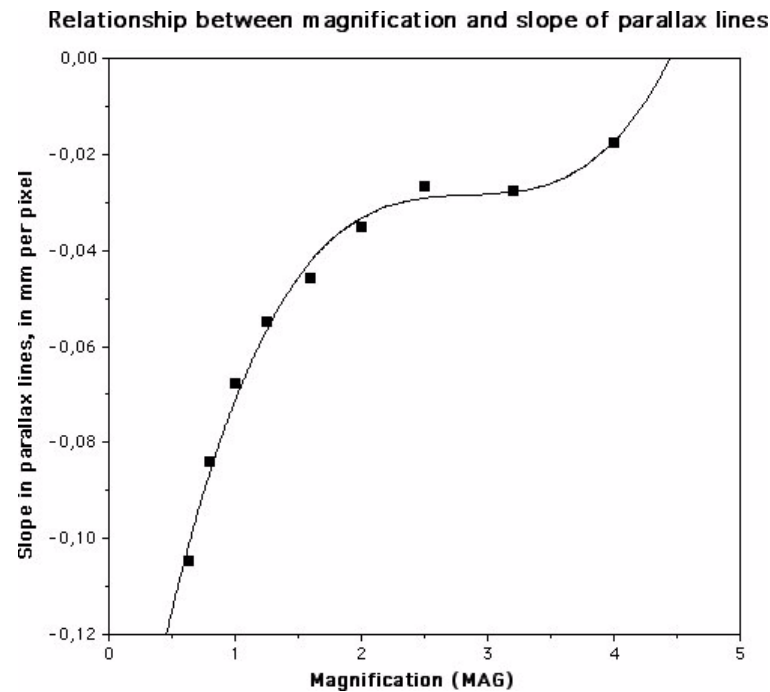

Figure 4. Influence of the microscope magnification on slope m of the parallax lines given in Equation 1 and illustrated in Figure 3. The equation of the cubic spline approximation (correlation coefficient 0.992) is $m = -0.18119 + 0.15946 * MAG - 0.055801 * (MAG)^2 + 0.0065467 * (MAG)^3$.

and to calibrate the microscope-camera-computer system. ImageJ 1.23 was used to align the stereo RGB images for movies. NIH-Image and ImageJ 1.23 are in the public domain and can be downloaded from National Institute of Mental Health at the URL http://rsb.info.nih.gov/nih-image/. For depth of focus enhancement the macro ExtendFocus was applied, which is part of the public-domain program Object-Image written by Norbert Vischer at the University of Amsterdam. Object-Image is an extended version of NIH Image and is available from http://simon.bio.uva.nl. The ExtendFocus macro is located at http://simon.bio.uva.nl/object-image.html [Note: Follow the download link DOC+Examples.sea.hqx. The macro is in the folder called macros.] Creation of anaglyphs (= overlays of stereo-pair images in a red and a green channel) was done with Adobe Photoshop 4.0 [Note: Anaglyphs can also been constructed in ImageJ or any other image processing software capable of handling multiple channel images.]. The construction of movies was accomplished with Quick-Time Virtual Reality Authoring Studio from Apple Computers, Inc.

MONO AND STEREO VISION, AND THE CONSTRUCTION OF ANAGLYPHS

In human vision each eye records the same scene under slightly different viewing angles. The difference in view between left and right eyes is called parallax and depends inversely on the distance of an object from the eyes. Through daily training this differential vision is continuously combined in the brain with our experience for close and far distances. This processing enables us to estimate distances and finally leads to a single virtual-stereo impression. In the subsequent text I use the term "mono-vision" for situations in which a scene or an object is viewed by one single sensor, and "stereo-vision" for cases where the object is seen by combining a pair of images with a parallax displacement (stereo-pair images).

In stereo-pair images the left and right image do not entirely match, but show double contours of most objects. This is essential for spatial vision because the displacement of the contours contains information about the distance of the object from the eye. The stereo-effect can be induced from such superpositions when anaglyphs are constructed and then watched with red-green glasses (anaglyph glasses). An anaglyph image is obtained when each image of a stereo-pair is shaded in different transparent colors (e.g., red and green) and then superposed. When observed with corresponding anaglyph glasses, a stereo impression emerges. The effect is explained by the fact that the eye watching through the red glass recognizes only the red portion of the image (the green image is filtered out and becomes black), while the other eye watching through the green glass recognizes the slightly displaced green portion of the image (the red image becomes extinct). This differential vision is neuronally combined to a three-dimensional perception. Anaglyph glasses are widely available for example from http://www.3d-brillen.de/.
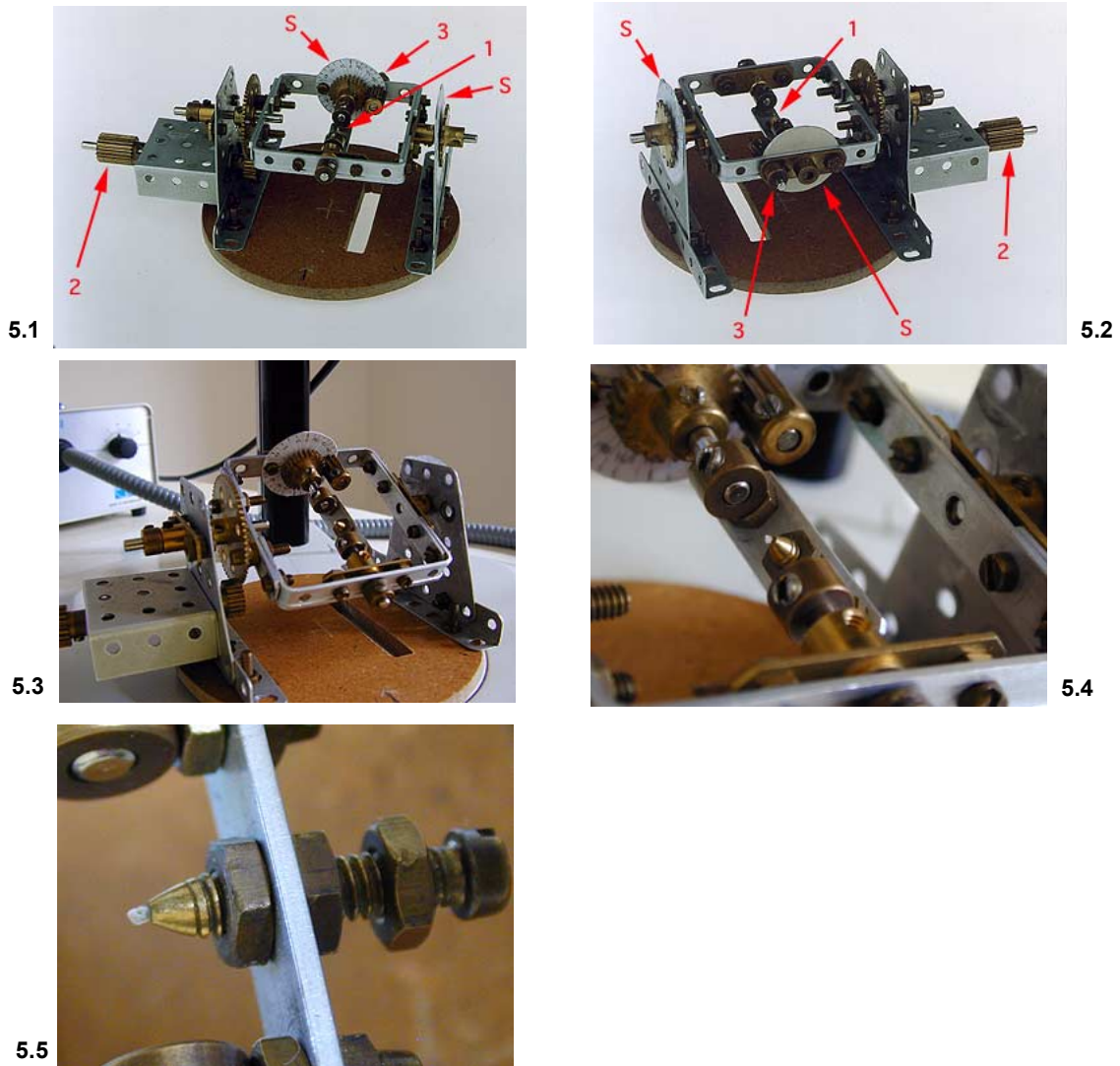
Figure 5. Universal stage for microfossils in front view (**5.1**) and back view (**5.2**). Arrow 1 points to the tip of a screw, where the specimen is mounted (see figures **5.3** to 5.5 for more details). The screw can be adjusted so that the specimen becomes eucentric with respect to the optical system of the microscope. Arrows 2 and 3 indicate the knobs to tilt in *y* and *x* directions, respectively. Arrows S indicate goniometric scales for tilt control (10° intervals). **5.3.** Gears for precise tilting in *x* and *y* directions. **5.4.** Foraminiferal specimen mounted on tip of screw. **5.5.** Screw for fine adjustment into eucentric position, so that the specimen does not move out of focus during tilt in *x* and *y* directions.
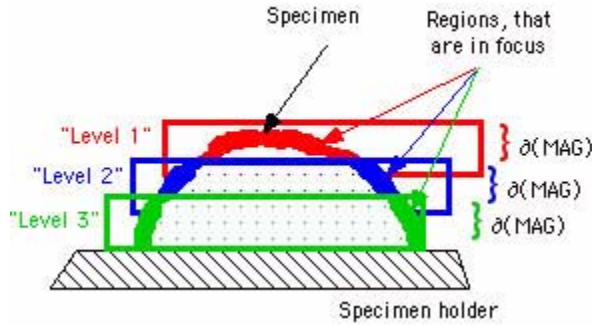
METHODS

In the following sections the procedures leading to animations in stereo vision at improved depth of focus are described in three steps:
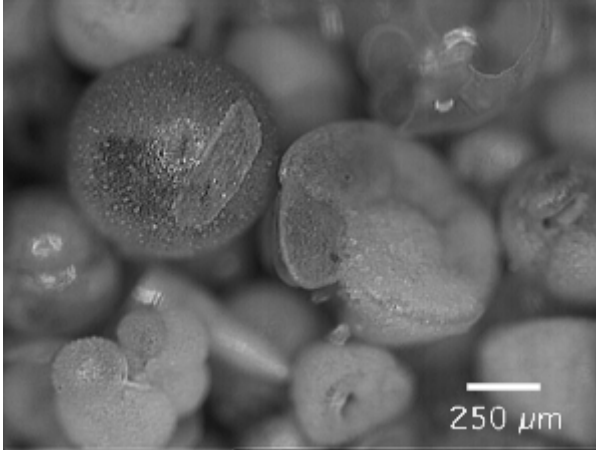
- depth of focus enhancement (Fusing method),
- construction of stereo images, and
- construction of virtual reality objects.

Fusing Method: Generation of Images with Extended Depth of Focus in Mono-Vision:
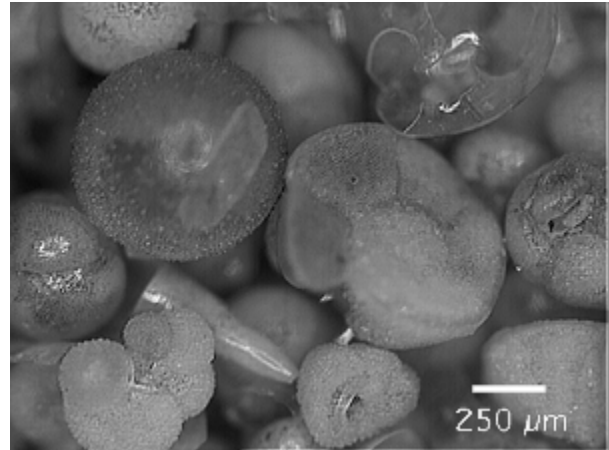
Reduced depth of field is a physical limitation in light optical microscopes. With the help of computer-aided microscopy this difficulty can be circumvented by separating out the sharp regions in a stack of digital images from several focal planes and then re-combining them to a composite with extended depth of focus. In practice these focal levels are not planes but are rather 'focal volumes' with the heights being equal to the depth of focus (e.g., Fig. 6.1). Any surface that intersects this volume appears as a sharp image. The depth of
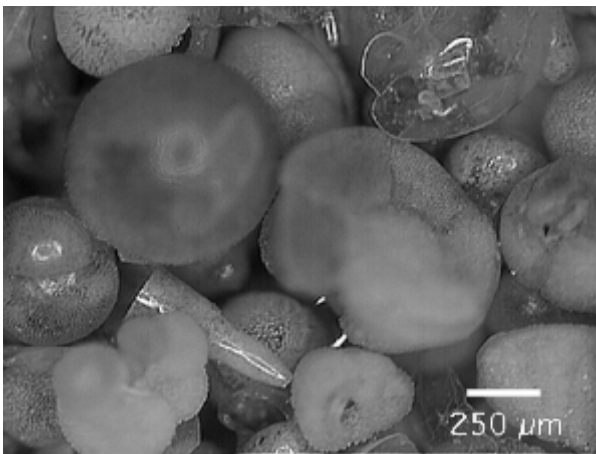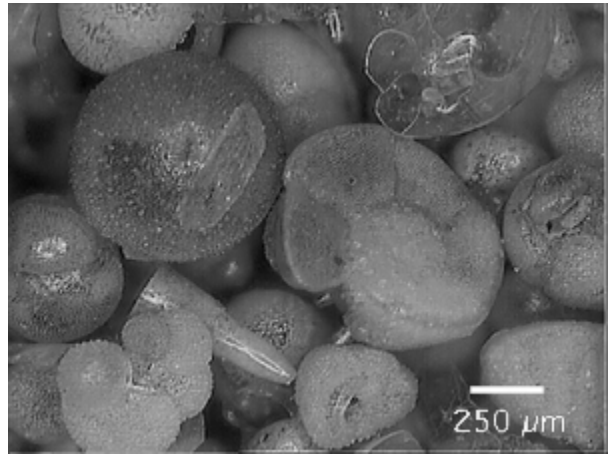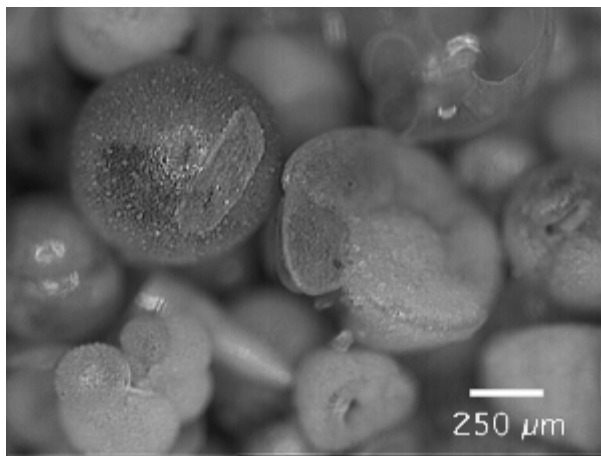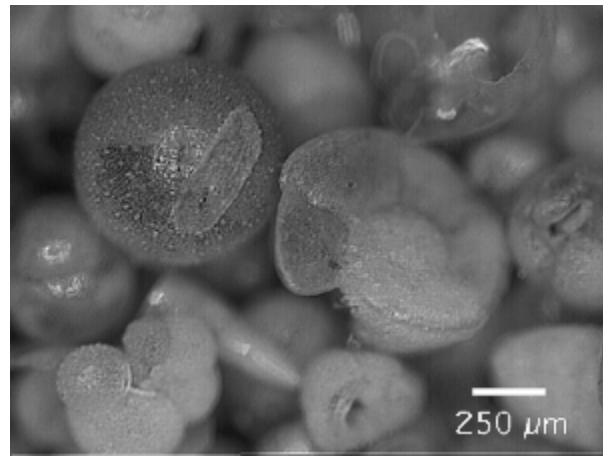
6.1

6.2

6.3

6.4

6.5

Figure 6. Fusion method. **6.1:** diagrammatic representation of three focal volumes, that intersect a specimen at levels 1 to 3. The height d of a particular focal volume represents the depth of focus and is a function of the magnification. Figures **6.2** to **6.4:** examples of images taken at three subsequent focal planes. Note various regions with changing sharpness as one focuses from top to down. The images were taken in the monoscopic mode position (=left light beam of the microscope). Figure **6.5:** resulting 'fused' image with extended focus after application of the FocusExtend macro. The images show shells of Recent planktonic foraminifera from surface sediment sample Ki 04, 0-1.5 cm, (Western Mediterranean Sea, lat. 37° 30' N, long. 7° 21' E, water depth 2756 m, taken during French oceanographic expedition VICOMED I in 1986, see Knappertsbusch (1993) for reference). Figures 6 through 9 were constructed from this sample. **6.1.** 'Focal volumes' seen in Figs. 6B-D. **6.2.** Upper focal plane (Level 1, left). **6.3.** Middle focal plane (Level 2, left). **6.4.** Lower focal plane (Level 3, left). **6.5.** Fused left image with extended focus.

7.1   **7.2**

Figure 7. Stereo-pair images from focus level 1 (upper level) illustrated in Figure 6. **7.1** is the left image (taken in the monoscopic or coaxial position) and **7.2** is the right image (taken in the stereoscopic position of the microscope. **7.1** Left image of stereo-pair. **7.2.** Right image of stereo-pair.

focus, δ, is an inverse function of the magnification or the numerical aperture of the lens system (Shillaber 1944). At high magnifications or at high numerical apertures, δ is small and at low magnifications or low numerical apertures, δ is large. When the focal volume is idealized to a focal plane, the image content from the focal volume can be considered as the integral of gray-level variation across the depth of focus per pixel.

Considering focal planes in this simplified manner, the sharp areas in a focal plane can be identified by calculating the local sharpness, which is the variability of gray levels in a selected subregion of a digital image (variance of gray levels or the difference between maximum and minimum gray levels in a region of interest). In order to detect a sharp region by gray-level variation color or shading effects in the original image must first be removed, which is done by generation of a gradient image (for example with a Sobel convolution filter). The sharp region appears then as an area with a high frequency of gray-level variation, while a blurred or unsharp region displays low variability in gray levels.

These principles are implemented in the NIH-Image macro 'Focus Extend', which was applied in this study. Images were acquired by moving the microscope body to a 'mono-mode' (= coaxial) position and taking gray-level images at three different focal levels (Figures 6.2-6.3). The three images were then fused into a single composite with extended focus (Fig. 6.5). The matching of images must be precise enough for image fusion otherwise edge effects will occur. Image alignment for each level was performed by identification of a small landmark, that remains visible throughout the entire stack. Using NIH-Image, Adobe Photoshop,

or any other image processing software, the images from the individual focal planes can be aligned in horizontal (x) or vertical (y) directions until the landmark has identical coordinates in all levels.

PREPARATION OF STEREO-PAIR IMAGES

Stereo-Vision without Correction for Depth of Focus

As described above, stereo-vision is obtained when two images of the same object are produced from slightly different angles of view, shaded with different colors, and then superposed. This was accomplished here by first producing a stereo-pair of gray-level images of the object at the same focal plane with NIH-Image. For this purpose the microscope was set to the "stereo-vision" position for taking the right image, and then moved sidewards to the left, to shoot the left image (Fig. 7). An anaglyph image was then produced using a graphics program capable of displaying color information in several channels (e.g., Adobe Photoshop, ImageJ). The left gray-level image was inserted into the red channel and the right gray-level image was inserted into the green channel of a new RGB-mode document, while the blue channel was changed to black. When recombining all channels (Fig. 8) the stereo-effect can be observed with red-green anaglyph glasses.

Stereo Vision with Correction for Depth of Focus

Improved stereographic vision for a microscopic object is obtained if the depth of focus enhancement is done in the left and right images of a stereo-pair. This was realized by first obtaining
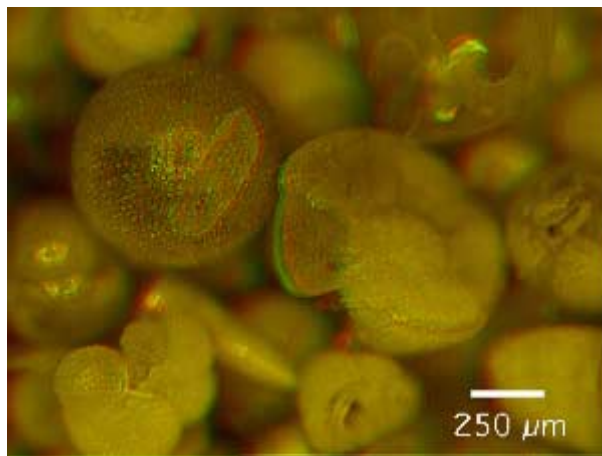
Figure 8. Anaglyph (=red-green) image of the (unfused) stereo image pair shown in Figure 7 (focus level 1). Use red-green glasses to experience the stereo-perception. The **Orbulina universa** (large sphere) and **Globorotalia truncatulinoides** (large specimen next to **O. universa**) are directed towards the observer, whereas the pteropod (elongate specimen below **O. universa**) is in the back.

stereo-images at several, pair-wise identical focal planes across the object. In a second step the NIH-Image macro ExtendFocus was applied to each of the left and right stack. Finally, the pair of fused images was combined into a single anaglyph for stereo-vision.

Because of the different geometry of the light paths in monoscopic mode (= left) and stereo-scopic mode (= right) position of the magnification changer body, two separate fusion procedures must be applied for the left and right images. In the monoscopic mode (left side), images taken from different focal planes need no or only little correction for the best overlap because the geometry of the light path through the microscope is coaxial. In the stereoscopic mode (= right side) position, images from the individual focal planes do not match because of the oblique light beam with respect to the optical axis of the microscope (see above). The offset of identical points (Dx) between different focal planes must be eliminated prior to the application of the focus extend macro. This was accomplished by selecting one of the images as a reference and shifting the remaining images by a constant amount until all images overlap completely. The correction can be accomplished either by manual determination of the offset using the x,y coordinates of a selected structure on the object that can be easily identified at all focal levels, or by calculation of the offset as a function of z using Equation (2). After alignment of the right images, the left and the right image stacks can be fused with the Focus Extend macro. The result is a pair of

stereo images at improved depth of focus, from which an anaglyph for stereo vision can be generated (see Section 2.1). Figure 9 illustrates these steps for the same example as shown in Figures 6 through 8.

Animated Sequences

Movie sequences were created with Quick-Time Virtual Reality Authoring Studio from a series of fused mono- and stereo images at stepwise varying angular positions of the specimen. Specimen orientation was performed with a universal eucentric stage, that was constructed for this purpose. The stage is small enough that it fits under the microscope and allows the user to tilt and rotate the specimen at equal intervals while the object remains in focus (i.e., without operating the focus control of the microscope). Focus-corrected images for mono- and stereo images were prepared for tilt intervals of 10° over an angular range of 270°. Within this range, the foraminifer can be watched from its spiral-, keel-, and umbilical sides without re-mounting the specimen. In the present example the individual images were resized at 400x400 pixels in order to minimize the size of the final VR file (for better performance when embedding it into a html document). In order to arrive at a precession-free movement, all images were aligned a second time with respect to a previously defined reference point on the shell. Determination of the necessary corrections in x and y directions was done with NIH-Image (for monoscopic vision) or ImageJ (for stereoscopic vision), and the image alignment was accomplished using Adobe Photoshop. Figures 10 and 11 show Quick-Time VR representations of the specimen in monoscopic and stereoscopic vision.

Discussion and conclusions

The described method is a powerful and inexpensive tool for generating close-range animated 3D stereo representations of microfossils next to existing visualization techniques for small objects. While previous methods of this type were derived from SEM images at full focal resolution, the present method was explicitly developed for use with light microscopy and limited depth of focus. Alternative techniques, such as SEM or X-ray computer tomography may lead to superior results, but these sophisticated technologies are expensive to acquire and maintain. Serial sectioning techniques for surface reconstruction purposes, as described by Sutton et al. 2001, represents another possibility, but is restricted currently to particle-size ranges of centimeters to a few millimeters. The methods
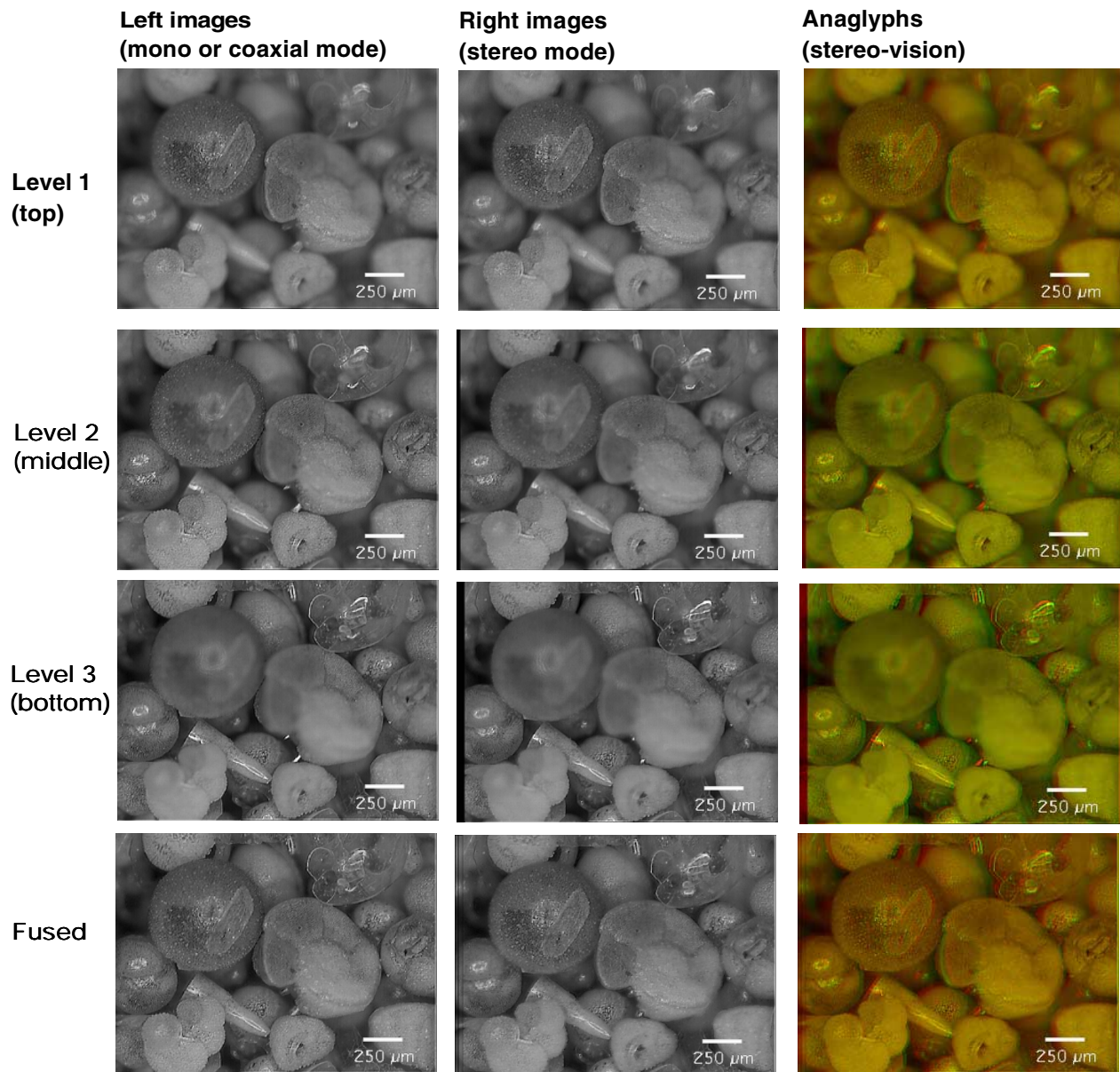
	Left images (mono or coaxial mode)	Right images (stereo mode)	Anaglyphs (stereo-vision)
Level 1 (top)			
Level 2 (middle)			
Level 3 (bottom)			
Fused			

Figure 9. Matrix of images showing the construction of focus improved anaglyph images. Horizontal rows represent focal planes 1 (top) through 3 (bottom). In the lowermost row are the results after application of the focus extend macro for levels 1 through 3. In the vertical columns are images taken in left (column 1) and right (column 2) positions of the microscope and the resulting anaglyphs for each level (column 3), respectively. The image shown in the lowermost row and in column 3 is the final result.

presented are still labour-intensive, but have potential for standard application if the individual steps can be automated and if the precision of the mechanical orientation control can be improved. The technique is especially suitable for the illustration of microfossil type specimens in 3D on the internet, in illustrated microfossil databases, in digital taxonomic atlases (e.g., for usage onboard research ships), for demonstration and teaching purposes, or to show the beauty of microfossils in public displays or museum exhibitions.

Figure 10. QuickTime movie of the planktonic foraminifer **Globorotalia menardii** in mono mode. By dragging the mouse pointer over the object it is possible to watch the shell from various sides (allow a few moments for your computer to load the image).

Figure 11. QuickTime movie of the planktonic foraminifer **Globorotalia menardii** in stereo mode. Use red-green anaglyph glasses to experience stereo vision. By dragging the mouse pointer over the object it is possible to view the shell from various sides (allow a few moments for your computer to load the image).

REFERENCES

Knappertsbusch, M. 1993. Geographic distribution of living and Holocene coccolithophores in the Mediterranean sea. *Marine Micropaleontology,* vol. 21, pp. 219-247.

Sutton, M. D., Briggs, D. E. G., Siveter, D. J. , and Siveter, D. J. 2001. methodologies for the visualization and reconstruction of three-dimensional fossils from the Silurian Herefordshire Lagerstätte. *Palaeontologia Electronica,* vol. 2, http://palaeo-electronica.org/2001_1/s2/issue1_01.htm.

Lyons, Patrick D. and Head, L. 1998. QuickTime VR: a powerful new illustrative tool for micropaleontological research. *Palaeontologia Electronica,* vol. 2, http://palaeo-electronica.org/1998_2/lyons/issue2.htm.

Ponce de Leon, M. S., and Zollikofer, Ch. P. 2001. Neanderthal cranial ontogeny and its implications for late hominid diversity. *Nature,* vol. 412, August 2001, pp. 534-538.

Shillaber, C. P. 1944. *Photomicrography in theory and practice.* John Wiley and Sons, Inc., London.

Zollikofer, C. P. E., Ponce de León, M. S., and Martin, R. D. 1998. Computer-assisted paleoanthropology. *Evolutionary Anthropology,* vol. 6, pp. 41-54.

Zollikofer, C. P. E., and Ponce de León, M. S. 2000. Computer-assisted paleoanthropology: new techniques and results. A*cta Anthropologica Sin.* (suppl.) vol. 19, pp. 90-97.

X-Ray microtomography: desktop high-resolution microtomography (from SkyScan): http://www.skyscan.be/